Present Status of the Applications of Pyroelectricity to the Detection of Far-Infrared Radiations

A. HADNI

Abstract—**The best detectivity at room temperature is obtained with a TGS single-crystal plate 10 μm thick: $D^*(47°C) = 6 \cdot 10^8$ W^{-1} $Hz^{1/2}$ cm. It is shown that epitaxial layers can give as good or better detectivities.**

I. INTRODUCTION

GOOD DETECTORS are needed for the development of submillimeter technology. The meaning of good detectors depends on the kind of experiments which are considered and it seems there is a place for thermal detectors operating at room temperature. For instance, in cases where the background is at room temperature there is not a great improvement in operating the detector at a low temperature, and the ideal background-limited detectivity is well known:

$$D_{\text{lim}}^*(300\ \text{K}) \simeq 3 \times 10^{10}\ \text{W}^{-1}\ \text{cm}\ \text{Hz}^{1/2}. \quad (1)$$

Among the many physical properties sensitive to temperature, the pyroelectricity of several materials is probably the most convenient to use and it has been widely employed for infrared detection during the past few years [2],[3]. A crystal is pyroelectric when the unit cell is lacking sufficient symmetry to get an electric dipole moment. The problem is to know how close the pyroelectric detector can approach the aforementioned ideal limit, and which are its potential applications.

II. DETECTIVITY OF A SINGLE PYROELECTRIC ELEMENT

Let us recall the result of a simple treatment of a pyroelectric detector [4]. The pyroelectric plate perpendicular to the pyroelectric axis (type I detector) has a surface area $A = L \times 1$ and a thickness d (Fig. 1). It is illuminated on its whole surface by a beam sine wave modulated at an angular frequency ω, and an electrical voltage S appears across the crystal:

$$S = \frac{E \Delta L_M \alpha \mathfrak{I} \lambda \omega R}{2\mathcal{G}} (1 + \omega^2\tau^2)^{-1/2}(1 + \omega^2\tau'^2)^{-1/2} \quad (2)$$

where ΔL_M is the amplitude of brightness modulation; E is the acceptance of the beam; α is the absorption coefficient of the detector; $\mathfrak{I}$ is the window transmission; $\lambda = (dP_s/dT)$ is the pyroelectric coefficient; $\mathcal{G}$ is the conductance per unit square area; $\tau = \mathcal{C}/\mathcal{G}$ is the thermal time constant; $\mathcal{C}$ is the thermal capacity per unit square area, $\mathcal{C} = c'd$, c' being the thermal capacity per unit volume; $1/R = 1/\rho + 1/\rho'$, ρ being the bias resistance and ρ' the internal resistance of the crystal; and $\tau' = RC$ is the electrical time constant, C being the electrical capacity of the crystal and $\tau' \ll \tau$.

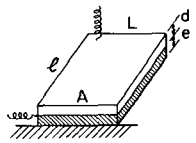

Fig. 1. Pyroelectric-detector element.

For low frequencies ($\omega^2\tau^2 < 1$ and $\omega^2\tau'^2 \ll 1$)

$$S \simeq \frac{1}{2\mathcal{G}} \Delta L_M \alpha \mathfrak{I} \lambda R \omega \quad (3)$$

while for high frequencies ($\omega^2\tau'^2 > 1$ and $\omega^2\tau^2 \gg 1$)

$$S \simeq \tfrac{1}{2} E \Delta L_M \alpha \mathfrak{I} \frac{\lambda}{\omega} \quad (4)$$

and Fig. 2 represents S versus ω in a range of frequency where R is assumed to be independent of ω. It is seen that responsivity decreases as $1/\omega$ when $\omega > \omega_2$.

The predominent noise B is Johnson noise which comes from the real part of the impedance Z of the whole detector $1/Z = jC\omega + (1/R)$, hence

$$B = 2(RkT\Delta f)^{1/2}(1 + \omega^2\tau'^2)^{-1/2}. \quad (5)$$

(For high frequencies, $B \simeq (2(kT\Delta f)^{1/2})/(R^{1/2}C\omega)$ is decreasing when either R or ω increases.)

Now detectivity $D^* = (S/B)(\Delta f^{1/2}(A)^{1/2})/(E\Delta L_M)$,

$$D^* = \alpha \mathfrak{I} \frac{\lambda \omega R^{1/2} d^{1/2}}{4\mathcal{G}} (1 + \omega^2\tau^2)^{-1/2}(kT)^{-1/2}(A)^{1/2}. \quad (6)$$

The detectivity is proportional to $R^{1/2}$ and is maximum for R maximum. We thus have to take $\rho \gg \rho'(\omega)$ and then $R \simeq \rho'$; $\rho' = \rho_0(d/A)$; now $\rho_0 = 1/(\epsilon_0\epsilon''\omega)$ and ϵ'' does not change with ω up to 1 MHz [5].

Hence

$$D^* = \frac{\alpha \mathfrak{I} d^{1/2} \omega^{1/2}}{(kT\epsilon_0)^{1/2} 4\mathcal{G}(1 + \omega^2\tau^2)^{1/2}}$$

and if $\omega^2\tau^2 \gg 1$,

Manuscript received June 20, 1974.
The author is with the University of Nancy, Nancy, France.

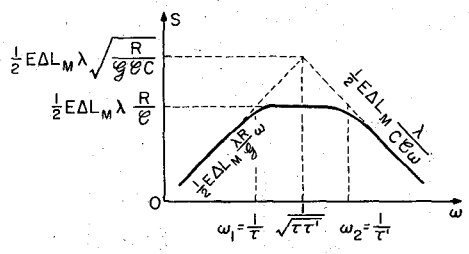

Fig. 2. Responsivity of a pyroelectric detector versus frequency in a range of frequency where R is assumed to be constant. (The bias resistance ρ is taken equal to the value of the crystal internal resistance ρ' at the highest frequency limit.)

$$D^* \simeq \frac{\alpha 3M(T)}{4(k\epsilon_0)^{1/2}d^{1/2}\omega^{1/2}} \tag{7}$$

where

$$M(T) = \frac{\lambda}{c'(\epsilon'' T)^{1/2}} \tag{8}$$

is a figure of merit of the pyroelectric detector.

We shall make two comments.

1) The frequency ω enters into (7) by its square root only, hence a slow decrease of detectivity when frequency increases, and this is one important advantage of pyroelectric detectors. For instance, the shape of laser pulses as short as 2 ns has been studied recently [6] with a pyroelectric detector having a time constant $\tau' = 0.3$ ns with $R = 50\ \Omega$ corresponding approximately to the resistance ρ' of the pyroelectric detector ($LiTaO_3$) for a 10^9-Hz frequency.

2) The figure of merit $M(T)$ is the highest for triglycine selenate [M (20°C) $\simeq 18\,000\ \mu C \cdot cm \cdot deg^{-1/2} \cdot J^{-1}$] and triglycine sulphate [M (47°C) $\simeq 5600$]. However, other pyroelectric materials, i.e., $LiTaO_3$, $Sr_{0.66}$, $Ba_{0.33}$, Nb_2O_3, etc., have been used which show higher λ and ϵ'' coefficients. They give a larger signal with a larger noise due to a smaller resistance [see remark after (5)] and this may be useful to keep signal noise larger than amplifier noise for high frequencies.

III. IMPROVEMENT BY REDUCING CRYSTAL THICKNESS

The obvious way to increase the detectivity is to decrease the crystal thickness. At a 5-Hz frequency with $d = 100\ \mu m$, D^* (100 μm, 47°C) $= 0.2 \cdot 10^9\ W^{-1}\ Hz^{1/2}$ cm, and for $d = 10\ \mu m$ we have obtained the highest detectability

$$D^* (10\ \mu m, 47°C) = 0.6 \cdot 10^9\ W^{-1}\ Hz^{1/2}\ cm. \tag{9}$$

This result is in good accordance with (7), and it is possible to calculate how thin the crystal ought to be to reach the ideal detectivity given by (1). For TGSe (20°C), we get $d \simeq 1\ \mu m$. Such a thickness is not attainable by grinding and polishing the crystal, but etching and epitaxial methods might be used. The problem then is to know if the pyroelectric properties are kept for such a thickness, and also if the absorption coefficient is still high enough.

We have made some measurements on a TGS layer 2 μm thick made by the spinning technique described by Jacob *et al.* [7]. The plate has been inspected by the pyroelectric probe technique [5] to know the dimensions of crystallites and their orientation (Fig. 3). About two-thirds of the crystal area have the right orientation to make a pyroelectric detector with the monoclinic axis perpendicular to the plate. This result is quite different from the assumption of Jacob *et al.* in terms of random orientation of the a and b axis within the film. For this thickness we have seen that most electric parameters keep their bulk values: spontaneous polarization P_s, pyroelectric coefficient λ, and dielectric constant. There is an exception for the coercive field which is one order of magnitude larger ($E_c \simeq 1.5$ MV/m). This is, of course, an advantage. From hysteresis loops we have measured an average $\bar{P}_s = 1.9\ C/cm^2$. Now $P_s = 2.7\ C/cm^2$ and then $(\bar{P}_s/P_s) = 0.7$ in good accordance with observed crystal plates orientation.

With a blackbody at 500 K, we have measured a detectivity $D^* \simeq 7 \cdot 10^7\ W^{-1}\ Hz^{1/2}$ cm, which is only one order of magnitude away from the best one. It could be improved by taking more care (the detector is not evacuated, and it is operated at 22°C, far away from the Curie temperature), and by a better orientation of the TGS layer. However, for very long wavelengths ($\lambda > 50\ \mu m$) the TGS layer optical thickness becomes smaller than a quarter-wavelength, and as it has to be stuck on a conductor, the component of the electrical field of the standing

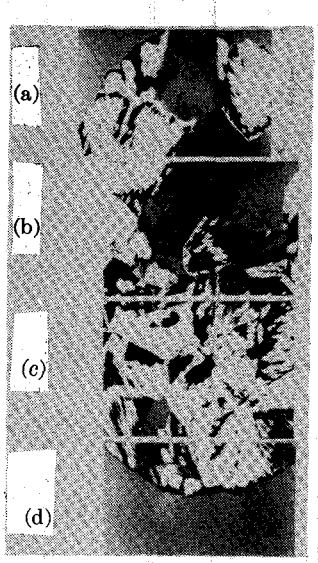

Fig. 3. Pyroelectric map of a TGS layer 2 μm thick showing a number of crystal plates with dimensions ranging around 300 μm. The grey ones in the middle of parts a and b cannot be turned into white or black by application of an electric field and have their monoclinic axis C_2 parallel to the surface. The other ones can be turned either into white or black by application of an electric field. This is evidence that they have their pyroelectric axis C_2 closely perpendicular to the surface. In the case of the photograph they are white and we see the nucleation of a number of black domain into them.

waves parallel to the plate is very close to zero both in TGS and in the absorbing thin-metal surface layer. The sensitivity of the usual geometric configuration might decrease drastically.

IV. APPLICATION OF TV PYRICON TUBES TO VISUALIZE FAR-INFRARED RADIATION

The last but not the least advantage of pyroelectric detectors is to provide a large-area retina for the thermal TV vidicon tube. The infrared image is projected onto the crystal surface and transformed into an electric image which is inspected by the electron beam [8]. Such a tube is now very useful in the laboratory to see far-infrared radiation [9] either from thermal sources or from lasers. For instance, Fig. 4 and Fig. 5 show, respectively, the photograph of a TEM_{00} and of a TEM_{10} mode from a 337-μm laser.

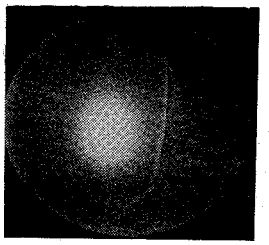

Fig. 4. Image of a TEM_{00} mode from an HCN laser (λ = 337 μm).

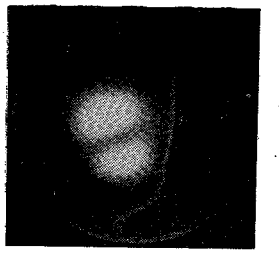

Fig. 5. Image of a TEM_{10} mode from an HCN laser (λ = 337 μm).

REFERENCES

[1] A. G. Chynoweth, "Dynamic method for measuring the pyroelectric effect with reference to barium titanate," *J. Appl. Phys.*, vol. 27, pp. 78–85, Jan. 1956.
[2] A. Hadni, "Possibilités actuelles de détection du rayonnement infrarouge," *J. Phys.*, vol. 24, pp. 694–702, Sept. 1963.
[3] A. Hadni, Y. Henninger, R. Thomas, P. Vergnat, and B. Wyncke, "Sur les propriétés pyroélectriques de quelques matériaux et leur application à la détection de l'infrarouge," *J. Phys.*, vol. 26, pp. 345–360, June 1965.
[4] A. Hadni, R. Thomas, and J. Perrin, "Sur la sensibilité d'un récepteur pyroélectrique d'infrarouge modulé entre 10 et 300.000 cps," *Compt. Rend.*, vol. 268, pp. 325–328, Jan. 1969.
[5] A. Hadni, "Thermal far infrared detectors," in *Proc. Symp. Submillimeter Waves.* (Polytechnic Inst. Brooklyn, Brooklyn, N. Y., Mar. 31, Apr. 1–2, 1970), pp. 251–256.
[6] C. B. Roundy and R. L. Byer, "Subnanosecond pyroelectric detector," *Appl. Phys.*, vol. 21, pp. 512–515, Nov. 1972.
[7] J. T. Jacob and K. L. Keester, *J. Vac. Sci. Technol.*, vol. 10, pp. 231–234, Jan./Feb. 1973.
[8] F. Le Carvennec and D. R. Charles, "Infrared pick up tube with electronic scanning and uncooled target," *Advan. Electron. Electron Phys., Suppl.*, vol. 33A, pp. 73–85, Apr. 1972.
[9] P. Felix, G. Moirou, J. Veron, J. Mangin, and A. Hadni, "Visualisation des radiations infrarouges," *Rev. Opt.*, to be published.

Recent Advances in Commercial Fourier Spectrometers for the Submillimeter Wavelength Region

R. C. MILWARD

Abstract—**A slow-scan "real-time" Michelson interferometer and a new rapid-scan interferometer using signal averaging techniques and fast Fourier transform (FFT) spectrum computation are described and compared. Typical performances of both instruments are illustrated.**

I. INTRODUCTION

CURRENT commercial submillimeter wave interferometric Fourier spectrometers [1] may be generally divided into two categories according to the speeds at which they operate—the "aperiodic" type in which interferograms are scanned slowly (<1 Hz), and the "rapid-scan" type in which interferogram signals are modulated in the audio-frequency domain 10 Hz–10 kHz.

In the slow-scan interferometer, detector signals are suitably smoothed by analogue methods so that the results of a single interferogram scan suffice for the spectrum computations, whereas in the rapid-scan interferometer, a number of consecutively scanned interferograms are usually co-added and averaged to augment signal/noise ratios to a satisfactory level, before the infrared spectrum is computed.

In each case, greatly different requirements are demanded of the interferometer scanner, and the speed and

Manuscript received June 3, 1974.
The author is with Polytec GmbH and Company, Karlsruhe-Reichenbach, Germany.